

Research Article

Physicochemical Study of Photocatalytic Activity of TiO₂ Supported Palygorskite Clay Mineral

Lahcen Bouna,¹ Benaissa Rhouta,¹ and Francis Maury²

¹ *Laboratoire de Matière Condensée et Nanostructures (LMCN), Faculté des Sciences et Techniques Guéliz, Université Cadi Ayyad, BP 549, 40 000 Marrakech, Morocco*

² *CIRIMAT, Université de Toulouse, CNRS-UPS-INP, ENSIACET, 4 allée Emile Monso, BP 44362, 31030 Toulouse Cedex 4, France*

Correspondence should be addressed to Francis Maury; francis.maury@ensiacet.fr

Received 8 February 2013; Accepted 28 March 2013

Academic Editor: Christos Trapalis

Copyright © 2013 Lahcen Bouna et al. This is an open access article distributed under the Creative Commons Attribution License, which permits unrestricted use, distribution, and reproduction in any medium, provided the original work is properly cited.

This study deals with the influence of physicochemical parameters, namely, the photocatalyst loading, dye concentration, and pH of polluted solutions, on the degradation efficiency of Orange G (OG) solutions containing TiO₂ nanoparticles supported on palygorskite clay mineral (TiO₂-Pal). The TiO₂ photocatalyst attached to natural palygorskite fibers was elaborated by colloidal sol-gel route. It exhibits the anatase structure that is the most photoactive crystallographic form. The highest performances of supported photocatalyst on OG degradation were found using an optimum amount of TiO₂-Pal around 0.8 g·L⁻¹, which corresponds properly to *ca.* 0.4 g·L⁻¹ of TiO₂. This amount is interestingly lower than the 2.5 g·L⁻¹ generally reported when using pure unsupported TiO₂ powder. The photodegradation rate increases by decreasing OG initial concentration, and it was found significantly higher when the OG solution is either acidic (pH < 4) or basic (pH ≈ 11). For OG concentrations in the range 5 × 10⁻⁶–5 × 10⁻⁴ M, the kinetic law of the OG degradation in presence of TiO₂-Pal is similar to that reported for unsupported TiO₂ nanopowder. It follows a Langmuir-Hinshelwood model with a first-order reaction and an apparent rate constant of about 2.9 × 10⁻² min⁻¹.

1. Introduction

Heterogeneous photocatalytic oxidation recently has emerged as an efficient alternative process for wastewater treatment [1–5]. The principle of this technique relies on the creation of reactive species as holes (h⁺) and hydroxyl radicals (OH[•]) upon irradiating a semiconductor oxide with an energy source (hν) higher than its energy band gap [1, 5]. In optimized processes, the reactive species so-generated are able to induce complete mineralization of organic pollutants into CO₂ and H₂O [1]. TiO₂ anatase is the most active semiconductor oxide in photocatalysis and is besides widely used owing to its numerous advantages, namely, nonharmfulness, low cost, and chemical inertness [1]. However, its use in the form of nanopowder (e.g., commercial Degussa P25 powder) raises several problems such as agglomeration of the particles during the process, which reduces photocatalytic efficiency. Additionally, recovering of micron sized aggregated particles from water decontaminated by TiO₂ slurry needs to implement costly microfiltration processes [1, 4, 6, 7]. To

overcome these drawbacks, researches focus on improving photocatalytic activity by the development of TiO₂ supported photocatalysts in particular starting with natural materials as support.

Among the support materials envisaged, clay minerals are considered promising owing to their interesting inherent properties as their adsorption capacity, high surface area, multiscale porosity, and ability to be bound to chemical compounds [6–9]. In this respect, we reported recently the immobilization of TiO₂ anatase nanoparticles (NPs) with an average size of 10 nm onto particle surfaces of beidellite [10] and fiber surfaces of palygorskite [11] via a colloidal sol-gel route. Beidellite and palygorskite were both natural clay minerals sampled in Morocco from Agadir basin and Marrakech High Atlas regions, respectively. They were purified, characterized, and functionalized to be used as catalytic support [12, 13]. Preliminary photocatalytic tests for the degradation of Orange G dye (OG) were promising. In comparative tests with Degussa P25 powder, the TiO₂-Pal photocatalyst exhibited a higher activity.

Because the optimization of experimental conditions is very important in designing a slurry reactor for effective and efficient use [4], we have investigated in the present work the effects of physicochemical parameters on photocatalytic activity of TiO_2 supported palygorskite fibers in order to find out the best conditions permitting an efficient removal of OG dye. This pollutant was selected as model compound because it is widely used in the textile industry.

2. Experimental Details

2.1. TiO_2 Supported Palygorskite Photocatalyst. The principle of the synthesis method is first to modify palygorskite with surfactant to afford an organophilic functionalization advantageous to the hydrolysis and polycondensation of titanium precursor. Thus, upon annealing, the amorphous hydroxoxo Ti-based thin film grafted on the palygorskite surface is converted into TiO_2 nanoparticles uniformly distributed onto palygorskite fiber surfaces with a high conformal coverage.

In summary, TiO_2 supported palygorskite composite material (labeled TiO_2 -Pal) was prepared starting from Na^+ -exchanged purified palygorskite (Na^+ -Pal) isolated from raw clay picked up in Marrakech High Atlas region (Morocco) [11]. The supported photocatalyst was elaborated according to a colloidal sol-gel procedure in two steps described in detail elsewhere [11]. Briefly, the synthesis route first involved the preparation of organopalygorskite (CTA^+ -Pal) by ion exchange of Na^+ -Pal aqueous dispersion (1 wt.%) with 0.2 g of hexadecyltrimethylammonium bromide (CTAB). Thereafter, 5 cm^3 of titanium tetraisopropoxide (TTIP) in isopropanol was added to 1 g of CTA^+ -Pal dispersed in 7 cm^3 of isopropanol, and it was hydrolyzed by adding some water droplets, and afterwards it was condensed to give rise to the gel precursor CTA^+ -Pal-Ti. Thereafter, the annealing at 600°C for 1 h converted CTA^+ -Pal-Ti into TiO_2 -palygorskite nanocomposite (TiO_2 -Pal).

TEM and *in situ* XRD versus temperature analyses demonstrated the good conformal coverage and wrapping of palygorskite fibers with remarkably stable TiO_2 anatase NPs that exhibited an average size of *ca.* 10 nm (Figure 1) [11].

2.2. Photocatalytic Tests. The photocatalytic activity was evaluated by measuring the decomposition rate of Orange G (OG) aqueous solutions containing a dispersion of the supported photocatalyst. The degradation reaction was carried out in a batch quartz reactor ($40 \times 20 \times 36 \text{ mm}^3$) placed in a thermostated chamber (25°C) under the UV light of a lamp (HPLN Philips 125 W) emitting at 365 nm. The reactor was irradiated with a photon flux of $1 \text{ mW}\cdot\text{cm}^{-2}$ by adjusting the distance to the lamp so that it simulates the UV intensity of solar spectrum on the earth [14]. This lamp was chosen because the OG absorption is negligible at this wavelength and, as a result, the direct photolysis of the OG aqueous solution (without photocatalyst) was found negligible for more than 24 h. The dispersion was agitated with an inert Teflon magnetic stirrer.

Even though the OG dye adsorption is generally negligible on our clayey materials, the photocatalyst dispersed in

OG aqueous solution was first cautiously kept in the dark inside a thermostated chamber for approximately 1 h before starting the irradiation with UV light. To determine the dye concentration, aliquots were taken from the mixture at regular time intervals and centrifuged at 12 500 rpm for 5 min. The OG concentration in the supernatant was determined by measuring the absorbance at 480 nm using a UV-VIS-NIR spectrophotometer (Perking Elmer lambda 19) and by applying Beer-Lambert's law. More details on this test are reported in [15].

3. Results and Discussion

3.1. Influence of Photocatalyst Amount. Figure 2 depicts the variation of OG concentration versus irradiation time upon photocatalytic tests without and in presence of different amounts of TiO_2 -Pal nanocomposite. In the absence of the photocatalyst, the OG concentration remains constant confirming that OG photolysis is quite negligible using our UV source. In the presence of supported photocatalyst, the removal of OG is confirmed by the decrease of its concentration when irradiation time increases. This degradation tends to be even more important as the photocatalyst amount increases. For instance, 96% of OG has been removed from a 10^{-5} M aqueous solution after 90 min using $1.5 \text{ g}\cdot\text{L}^{-1}$ of supported photocatalyst. This is more clearly shown by depicting the initial rate (R_i) deduced from the slope of linear parts in the early stages versus photocatalyst amount (Figure 3) in agreement with a pioneering report [1]. Indeed, below a photocatalyst amount of *ca.* $0.5 \text{ g}\cdot\text{L}^{-1}$, the initial degradation rate of OG increases with the increase of supported photocatalyst concentration. This reveals a heterogeneous catalytic regime [1]. However beyond $0.5 \text{ g}\cdot\text{L}^{-1}$, the initial degradation rate of OG reaches a plateau and becomes independent of photocatalyst quantity.

Another illustration reveals a critical amount of the supported photocatalyst; this is the influence of the photocatalyst quantity on the time required to degrade for instance 60% of OG ($t_{60\%}$). Figure 4 reveals that below $0.8 \text{ g}\cdot\text{L}^{-1}$ the $t_{60\%}$ time decreases by increasing the amount of photocatalyst and it practically stabilizes beyond this threshold value. This indicates that even if the initial degradation rate R_i does not vary significantly for catalyst amount ranging from 0.5 to $0.8 \text{ g}\cdot\text{L}^{-1}$ (Figure 3), the photocatalytic efficiency still increases with the catalyst amount up to the critical quantity of $0.8 \text{ g}\cdot\text{L}^{-1}$ (Figure 4). For nanocomposite amounts lower than $0.8 \text{ g}\cdot\text{L}^{-1}$, the increase of OG photodegradation with the catalyst amount could be explained by a photons flux in excess with respect to the specific surface area of particles dispersed in the reacting media so that all the TiO_2 -Pal particles are exposed to radiation. However, for higher photocatalyst amounts ($>0.8 \text{ g}\cdot\text{L}^{-1}$), both shadowing effects can occur and particles can aggregate which in turn reduces the interfacial area between the solution and the photocatalyst. Thus the number of active sites on the catalyst surface is decreased [16]. In other words, an excess of particles results in a screening effect masking part of the photosensitive surface [1] and increases opacity of the solution and

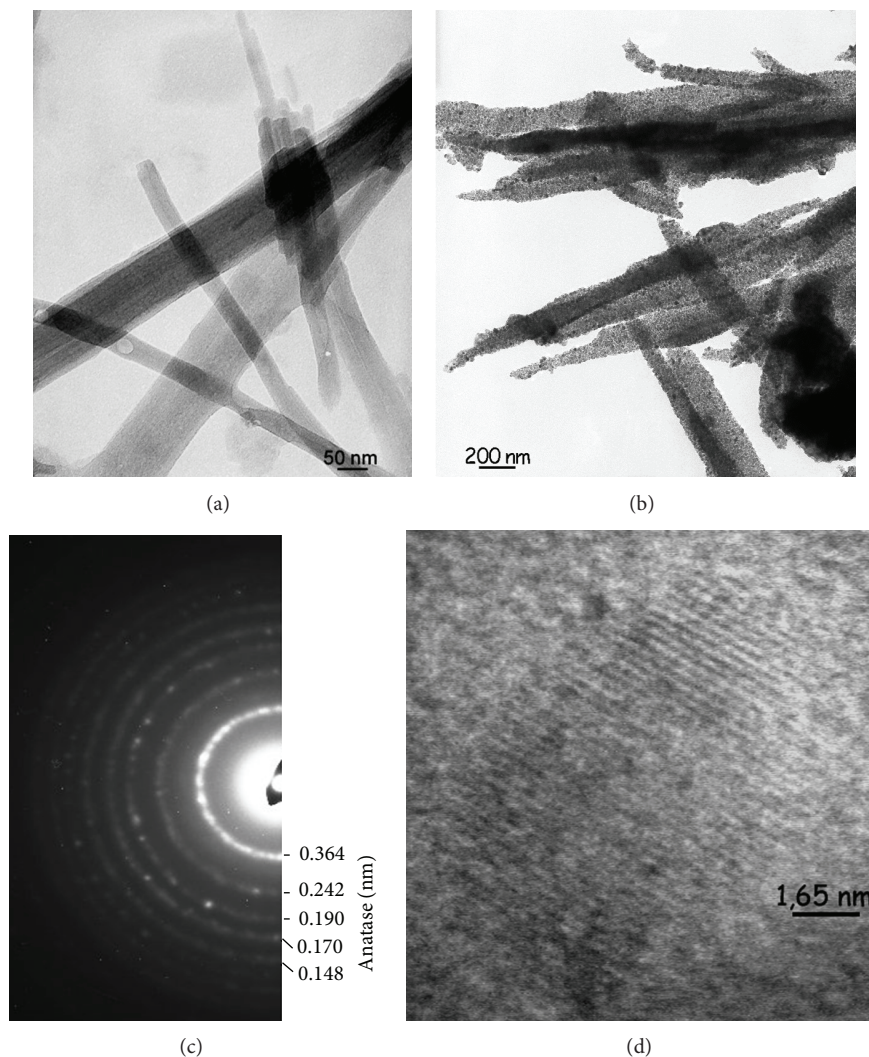


FIGURE 1: TEM micrographs of pristine palygorskite Na^+ -Pal (a) and TiO_2 -Pal (b) samples. Selected area electron diffraction pattern indexed with anatase (c) of a TiO_2 -Pal sample and high resolution electron micrograph (d) showing a nodular anatase NP (8–12 nm in diameter) and the $\{101\}$ planes with a reticular distance of *ca.* 0.3 nm [11].

light scattering [16] yielding to lower degradation rate of OG.

ICP analysis of TiO_2 -Pal supported photocatalyst gave a TiO_2 content of *ca.* 47 wt.%. Therefore, the optimum concentration of nanocomposite TiO_2 -palygorskite photocatalyst determined herein at $0.8 \text{ g}\cdot\text{L}^{-1}$ properly corresponds to $0.37 \text{ g}\cdot\text{L}^{-1}$ of TiO_2 attached to palygorskite fibers, since the nanocomposite contains 47 wt.% of anatase. This TiO_2 amount of *ca.* $0.4 \text{ g}\cdot\text{L}^{-1}$ is significantly lower than the optimum concentration ($2.5 \text{ g}\cdot\text{L}^{-1}$) previously reported in the case of unsupported TiO_2 slurry [1]. Interestingly this result indicates that photodegradation efficiency could be achieved with lower amount of TiO_2 when it is immobilized onto palygorskite fibers in comparison with which is required for unsupported TiO_2 .

The time dependence of logarithmic plot $\log(C_0/C)$ corresponding to the degradation of an OG solution (10^{-5} M) with a TiO_2 -Pal catalyst loading of $1 \text{ g}\cdot\text{L}^{-1}$ reveals a linear

variation (Figure 5). This behavior is similar to that of unsupported TiO_2 powder slurry and suggests a first-order reaction. The apparent rate constant deduced from the slope is around $2.9 \times 10^{-2} \text{ min}^{-1}$.

3.2. Influence of Initial OG Concentration. Figure 6 shows OG degradation curves as a function of initial dye concentration using a TiO_2 -palygorskite loading of $1 \text{ g}\cdot\text{L}^{-1}$. It is shown that the lower the initial dye concentration, the faster the OG removal. Indeed, after 75 min of irradiation, a total OG degradation is observed for a $5 \times 10^{-6} \text{ M}$ solution, while only 87%, 83%, and 57% of OG degradation were recorded for initial dye concentration of 10^{-5} , 3×10^{-4} , and $5 \times 10^{-4} \text{ M}$, respectively. As beforehand evidenced, OG photolysis is negligible (Figure 2). Therefore, the decrease of OG photodegradation by increasing its initial concentration could be explained by significant absorption of photons flux by the dye. Photocatalysis is a heterogeneous process that

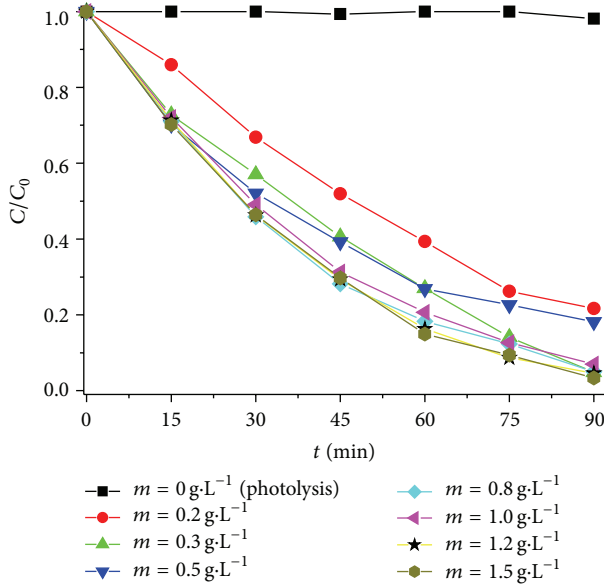


FIGURE 2: Influence of the supported photocatalyst amount on photocatalytic activity of TiO_2 supported palygorskite on the removal of Orange G from aqueous solution. OG degradation is given by its concentration at different time (C) divided by its initial concentration ($C_0 = 10^{-5}$ M).

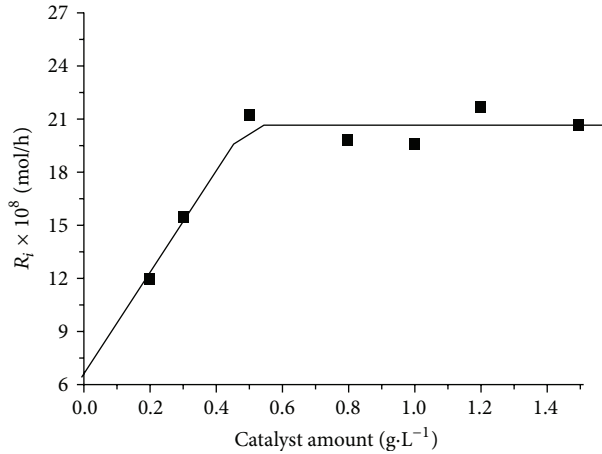


FIGURE 3: Variation of initial rate (R_i) of OG photodegradation versus the supported photocatalyst amount.

requires the combination of both photons and adsorption on catalytic sites. If photons flux decreases on the surface of supported photocatalyst due to absorption by the dye solution the efficiency of electron-hole photogeneration will also decrease and subsequently the formation of the required highly oxidant species, for example, OH^\bullet and $\text{O}_2^{\bullet-}$, will be reduced at the surface of photocatalyst [16].

Moreover, the photocatalysis kinetics generally follows a Langmuir-Hinshelwood mechanism with a reaction rate (R) varying proportionally with the coverage θ according to [1, 4]:

$$R = k\theta = k \left(\frac{KC}{1 + KC} \right), \quad (1)$$

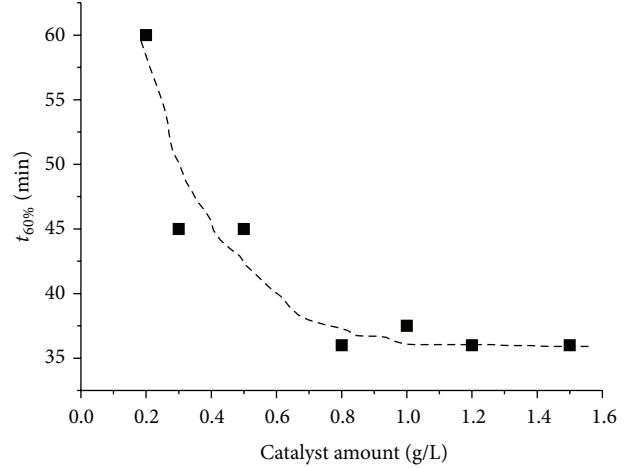


FIGURE 4: Influence of the supported photocatalyst amount on the time required to degrade 60% of OG ($t_{60\%}$).

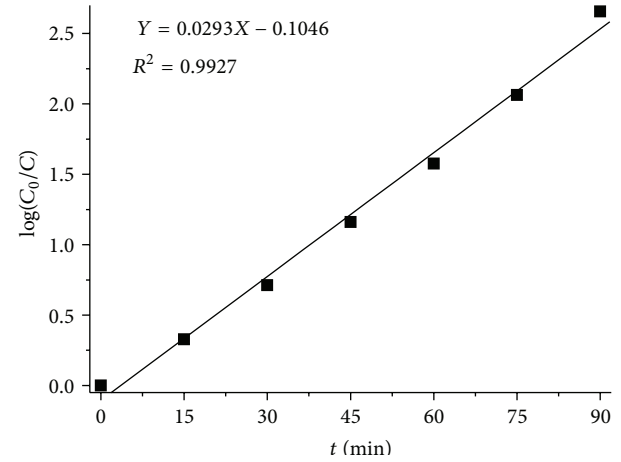


FIGURE 5: Logarithmic variation of OG relative concentration versus UV illumination time determined for a TiO_2 -supported palygorskite loading of $1 \text{ g}\cdot\text{L}^{-1}$ ($C_0 = 10^{-5}$ M).

where C is the pollutant concentration, k the rate constant, and K the equilibrium constant. Hence, the number of available catalytic sites decreases as the dye concentration increases, which in turn reduces OG photodegradation rate. As all OG solutions considered herein are diluted ($C < 10^{-3}$ M), the term KC becomes $\ll 1$ and consequently $R = k \cdot K \cdot C$. The reaction between photogenerated electron-hole and OG species (supposed to control the process) has an apparent first order as beforehand evidenced (Figure 5) [1, 4].

3.3. pH Effect of the Solution. The pH effect on photocatalytic degradation rate of OG solution (10^{-5} M) containing $1 \text{ g}\cdot\text{L}^{-1}$ of TiO_2 -supported palygorskite was studied by varying the pH from 2 to 11 by adding NaOH (basic pH) or HCl (acidic pH) (Figure 7(a)). The dependency on the pH is more clearly shown in Figure 7(b). The initial degradation rate of OG is high both for acidic pH (< 4) and basic pH (≈ 11). For median

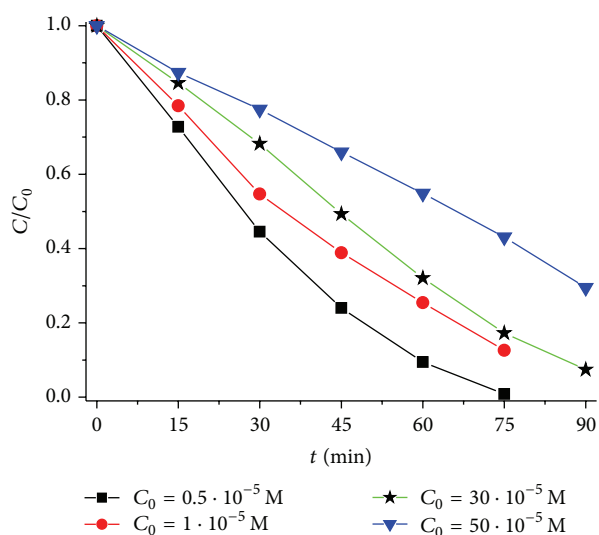


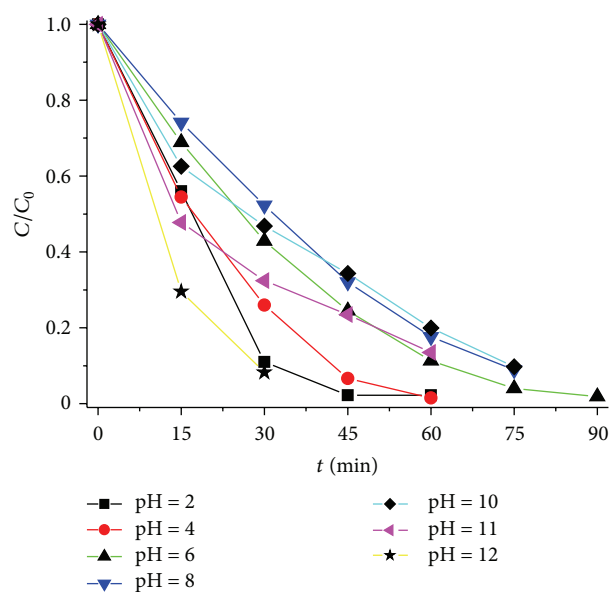
FIGURE 6: Influence of initial OG concentration on photocatalytic activity of $1 \text{ g}\cdot\text{L}^{-1}$ of TiO_2 supported palygorskite on the OG removal from aqueous solution.

values, the rate decreases by increasing pH from 4 to 8, then it increases to reach the highest level in the basic range.

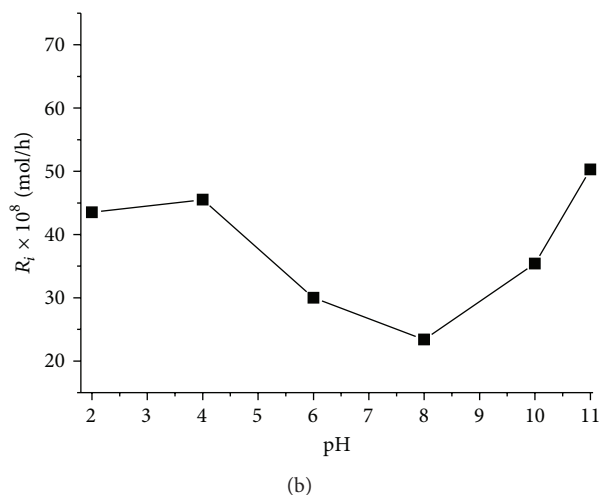
This may be ascribed to the pH effect on surface charge properties of TiO_2 nanoparticles wrapping palygorskite fibers (Figure 1). Indeed, in pH range 6–8, which includes the point of zero charge PZC (pH_{PZC}) of TiO_2 [17, 18], TiO_2 NPs surfaces are not charged, since they are mainly formed of neutral hydroxyl TiOH groups [19]. Hence, electrostatic interactions between particles are minimized and their agglomeration in the form of clusters is favored. This agglomeration reduces the transmission and absorption of light [20] and hence causes the decrease of dye degradation efficiency. Nevertheless, in strongly basic pH, TiO_2 nanoparticles surfaces are negatively charged in the form of TiO^- as a result of deprotonation of surface hydroxyl groups (TiOH) [19]. Consequently, electrostatic repulsions occur between particles, favoring their dispersion and hence the transmission and absorption of light which in turn enhance degradation rate of the OG dye. The same phenomenon likely occurs in acidic pH, but in this case, TiO_2 nanoparticles surfaces are positively charged in the form of TiOH_2^+ due to surface hydroxyls protonation [19]. In this case, besides the stability of TiO_2 -Pal dispersion, the adsorption of anionic species as OG molecules is likely much favored on positively charged surfaces sites of TiO_2 -Pal nanoparticles [21], which further improve the performance in photocatalysis.

4. Conclusion

This study shows that the photoactivity of TiO_2 NPs supported on palygorskite fibers depends on catalyst amount, OG dye concentration, and pH of the polluted solution. The photodegradation of OG was found to be the highest for an optimum photocatalyst loading of *ca.* $0.8 \text{ g}\cdot\text{L}^{-1}$. This corresponds to TiO_2 loading of only $0.37 \text{ g}\cdot\text{L}^{-1}$, which is significantly lower than literature data reported for unsupported



(a)



(b)

FIGURE 7: effect of pH: (a) photocatalytic OG degradation versus UV irradiation time as a function of the pH of aqueous solutions; (b) influence of pH of OG solutions on initial photocatalytic rate (R_i). The TiO_2 -Pal loading was $1 \text{ g}\cdot\text{L}^{-1}$ and initial OG concentration was 10^{-5} M .

TiO_2 nanopowders. The OG photocatalytic decomposition increases by decreasing the initial OG concentration of the polluted solution, and it is significantly improved by acidic and basic pH. These data are important to design and implement a slurry photoreactor and to determine its optimum operating conditions.

Acknowledgments

The financial supports from the “Convention de Coopération CNRST, Maroc/CNRS, France” (chemistry project no. 04/08), the “Programme de Coopération Scientifique Inter-universitaire de l’Agence Universitaire de la Francophonie”

(no. 63 13PS826), and the “Programme d’Action Intégrée Volubilis” (no. MA-08-185) are gratefully acknowledged.

References

- [1] J. M. Herrmann, “Heterogeneous photocatalysis: fundamentals and applications to the removal of various types of aqueous pollutants,” *Catalysis Today*, vol. 53, no. 1, pp. 115–129, 1999.
- [2] A. Fujishima, T. N. Rao, and D. A. Tryk, “Titanium dioxide photocatalysis,” *Journal of Photochemistry and Photobiology C*, vol. 1, no. 1, pp. 1–21, 2000.
- [3] Y. Paz, “Preferential photodegradation—why and how?” *Comptes Rendus Chimie*, vol. 9, no. 5-6, pp. 774–787, 2006.
- [4] O. Carp, C. L. Huisman, and A. Reller, “Photoinduced reactivity of titanium dioxide,” *Progress in Solid State Chemistry*, vol. 32, no. 1-2, pp. 33–177, 2004.
- [5] P. K. J. Robertson, “Semiconductor photocatalysis: an environmentally acceptable alternative production technique and effluent treatment process,” *Journal of Cleaner Production*, vol. 4, no. 3-4, pp. 203–212, 1996.
- [6] T. An, J. Chen, G. Li et al., “Characterization and the photocatalytic activity of TiO₂ immobilized hydrophobic montmorillonite photocatalysts. Degradation of decabromodiphenyl ether (BDE 209),” *Catalysis Today*, vol. 139, pp. 69–76, 2008.
- [7] P. Aranda, R. Kun, M. A. Martin-Luengo, S. Letaïef, I. Dékány, and E. Ruiz-Hitzky, “Titania-sepiolite nanocomposites prepared by a surfactant templating colloidal route,” *Chemistry of Materials*, vol. 20, pp. 84–91, 2008.
- [8] J. Liu, M. Dong, S. Zuo, and Y. Yu, “Solvothermal preparation of TiO₂/montmorillonite and photocatalytic activity,” *Applied Clay Science*, vol. 43, no. 2, pp. 156–159, 2009.
- [9] M. Nieto-Suárez, G. Palmisano, M. L. Ferrer et al., “Self-assembled titania-silica-sepiolite based nanocomposites for water decontamination,” *Journal of Materials Chemistry*, vol. 19, no. 14, pp. 2070–2075, 2009.
- [10] L. Bouna, B. Rhouta, M. Amjoud et al., “Synthèse, caractérisations et tests photocatalytiques d’un matériau argileux d’origine naturelle à base de la beidellite fonctionnalisée par TiO₂,” *Matériaux Et Techniques*, vol. 100, pp. 241–225, 2012.
- [11] L. Bouna, B. Rhouta, M. Amjoud et al., “Synthesis, characterization and photocatalytic activity of TiO₂ supported natural palygorskite microfibers,” *Applied Clay Science*, vol. 52, no. 3, pp. 301–311, 2011.
- [12] L. Bouna, B. Rhouta, L. Daoudi et al., “Mineralogical and physico-chemical characterizations of ferruginous beidellite-rich clay from Agadir basin (Moroc),” *Clays and Clay Minerals*, vol. 60, pp. 278–290, 2012.
- [13] E. Zatile, B. Rhouta, L. Bouna et al., “Comprehensive physicochemical study of dioctahedral palygorskite-rich clay from Marrakech High-Atlas (Morocco),” *Physics and Chemistry of Minerals*, 2013.
- [14] K. Hofstadler, R. Bauer, S. Novalic, and G. Heisler, “New reactor design for photocatalytic wastewater treatment with TiO₂ immobilized on fused-silica glass fibers: photomineralization of 4-chlorophenol,” *Environmental Science Technology*, vol. 28, no. 4, pp. 670–674, 1994.
- [15] C. Sarantopoulos, E. Puzenat, C. Guillard, J. M. Herrmann, A. N. Gleizes, and F. Maury, “Microfibrous TiO₂ supported photocatalysts prepared by metal-organic chemical vapor infiltration for indoor air and waste water purification,” *Applied Catalysis B*, vol. 91, no. 1-2, pp. 225–233, 2009.
- [16] M. Faisal, M. Abu Tariq, and M. Muneer, “Photocatalysed degradation of two selected dyes in UV-irradiated aqueous suspensions of titania,” *Dyes and Pigments*, vol. 72, no. 2, pp. 233–239, 2007.
- [17] A. Fernández-Nieves, C. Richter, and F. J. De Las Nieves, “Point of zero charge estimation for a TiO₂/water interface,” *Progress in Colloid and Polymer Science*, vol. 110, pp. 21–24, 1998.
- [18] L. A. García Rodenas, A. D. Weisz, G. E. Magaz, and M. A. Blesa, “Effect of light on the electrokinetic behavior of TiO₂ particles in contact with Cr(VI) aqueous solutions,” *Journal of Colloid and Interface Science*, vol. 230, no. 1, pp. 181–185, 2000.
- [19] C. Kormann, D. W. Bahnemann, and M. R. Hoffmann, “Photolysis of chloroform and other organic molecules in aqueous TiO₂ suspensions,” *Environmental Science and Technology*, vol. 25, no. 3, pp. 494–500, 1991.
- [20] W. Xi and S. U. Geissen, “Separation of TiO₂ from photocatalytically treated water by cross-flow microfiltration,” *Water Research*, vol. 35, no. 5, pp. 1256–1262, 2001.
- [21] L. Bouna, B. Rhouta, M. Amjoud et al., “Correlation between electrokinetic mobility and ionic dyes adsorption of Moroccan stevensite,” *Applied Clay Science*, vol. 48, no. 3, pp. 527–530, 2010.



Hindawi

Submit your manuscripts at
<http://www.hindawi.com>

